Advances in Science and Technology Research Journal

Advances in Science and Technology Research Journal 2022, 16(4), 1–9
https://doi.org/10.12913/22998624/152123
ISSN 2299-8624, License CC-BY 4.0

Received: 2022.06.09
Accepted: 2022.08.22
Published: 2022.09.01

Testing of Air-Cooling Efficiency of the Underside of a Turning Tool Carbide Insert in EN-GJL 250 Cast Iron Turning Operations

Marian Bartoszuk[1*], Mariusz Prażmowski[1], Igor Hurey[2,3]

[1] Faculty of Mechanical Engineering, Opole University of Technology, ul. Mikołajczyka 5, 45-271 Opole, Poland

[2] Faculty of Mechanical Engineering and Aeronautics, Rzeszow University of Technology, al. Powstańców Warszawy 12, Rzeszów 35-959, Poland

[3] Lviv Polytechnic National University, 12, Bandera st., 79013 Lviv, Ukraine

* Corresponding author's e-mail: m.bartoszuk@po.edu.pl

ABSTRACT

This article shows the results of research on the effectiveness of operation of an original tool air cooling system in cutting. A case of turning EN-GJL 250 cast iron with TH10 tungsten carbide cutting inserts without protective coatings was selected for testing. The paper gives constructional details of the tested tool cooling system and discusses the principle of its operation. The research carried out has shown that this way of cooling the cutting insert causes a significant decrease in temperature in all sub-areas of the cutting zone. In addition, air cooling has been proven to significantly reduce cutting tool wear and slightly improve the roughness of the machined surface. The results obtained showed that the proposed method of cooling can be successfully used in the treatment of grey cast iron. In the future, it may serve as a basis for the construction of a professional cooling system for industrial applications.

Keywords: cast iron machining, air-cooling system, cutting temperature, surface roughness, tool wear.

INTRODUCTION

As is well known during the cutting of metal materials, most of the energy is used to generate heat. This heat is generated by the plastic deformation of the workpiece material and by the friction between the cutting insert and chip as well as the cutting insert and the workpiece material. Heat in cutting is an unfavourable phenomenon, as it promotes wear of the cutting tool and, consequently, results in deterioration of dimensional accuracy of manufactured parts [1, 2]. Therefore, cooling of the cutting zone is commonly used to reduce the wear of cutting inserts. Low pressure (LP) coolant cooling is most commonly used, high-pressure cooling (HPC), ultra-high-pressure cooling (UHPC) and minimum quantity lubrication (MQL) are less frequently used [1, 3]. In recent years, however, environmental pressure has been increasing, which is why cooling with the use of a compressed gas medium and cryogenic cooling are gaining in popularity [1, 3, 4]. In some cases, how-ever, dry cutting is recommended [1, 4]. In this case, the solution to the problem of reducing the temperature of the cutting tool during the cutting process can be the so-called heat pipe [5, 6]. A heat pipe is a special, additional element introduced into the cutting zone. A heat pipe is usually made of copper, aluminium or other material with high thermal conductivity. At one end, it contacts the cutting insert and collects heat from it, then quickly distributes it throughout its volume and returns it to the environment. As Liang et al. [6, 7] have shown in their research, the heat pipe changes the distribution of heat fluxes in the cutting zone and reduces the tool-chip contact temperature. Liang et al. [6] have proved that the installation of a heat pipe increases the amount of heat entering the tool. At the same time, much more heat can be dissipated through the heat pipe and dispersed in the environment. It has been proven that a heat pipe can dissipate 36÷42% of all heat entering the tool. In other studies [7] Liang et al. have proven that the use of a heat pipe increases the effectiveness of heat dissipation from the entire cutting zone as the cutting speed increases. As a consequence, the temperature of the tool-chip contact area is reduced. The recorded drop in cutting tool temperature at this point is about 10%. It should be noted that in both studies [6, 7] the heat pipe comes into contact with a small area of the cutting edge (or adjacent area), but causes a decrease in temperature in the entire cutting area. Such a strong influence of the heat pipe is caused by the high thermal conductivity of the tungsten carbide which additionally in-creases with the temperature (Fig. 1).

In industrial practice, the solution of introducing an additional heat dissipating element into the cutting zone cannot always be applied. Often, simply put, there is no space to install a heat pipe. Moreover, sometimes a significant modification of the tool holder is required [9, 6]. For example, in the study by Quan and Mai [9] they used a modified tool holder, where a heat pipe was placed in a hole passing through a part of the tool holder and ending inside the cut-ting insert, directly adjacent to the tool-chip contact zone. An additional complication was that the heat pipe consisted of a thin copper pipe through which cooling water was pumped. The cooling system therefore required additional equipment in addition to the heat pipe, i.e. a thermostatic tank and water pump [9].

Focusing on the unquestionable advantages of heat pipe cooling systems, and we should mention here mainly the environmental performance and efficiency, the author made an attempt to build an alternative cooling system for the tool cutting tool. According to the author, such a system should use compressed air as a cooling medium in order to be environmentally friendly. Its design should be simple and should not require any significant modifications to the tool itself or the tool holder. In order to ensure effective cooling (similarly to a heat pipe) the carbide cutting insert and indirectly the tool shank should be cooled. It is assumed that the purpose of this cooling system will be to cool the cutting insert and not the chip or workpiece.

TEST METODOLOGY

A case of orthogonal cutting of EN-GJL 250 grey cast iron with uncoated TH10 carbide cutting inserts was selected for testing. The metallographic structure of workpiece material is shown in Figure 2. The tests were carried out using the CTGNR

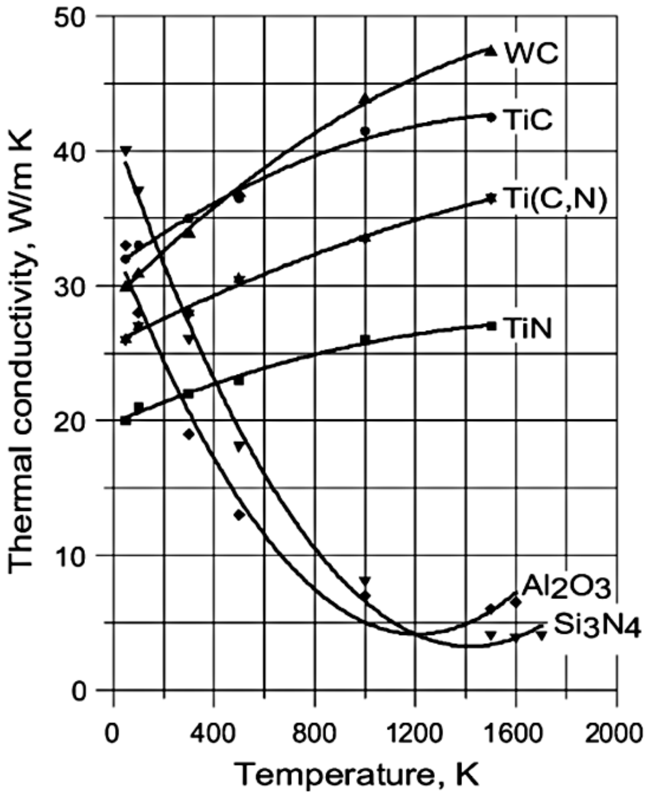

Fig. 1. Thermal conductivity of carbide and selected tool coatings [8]

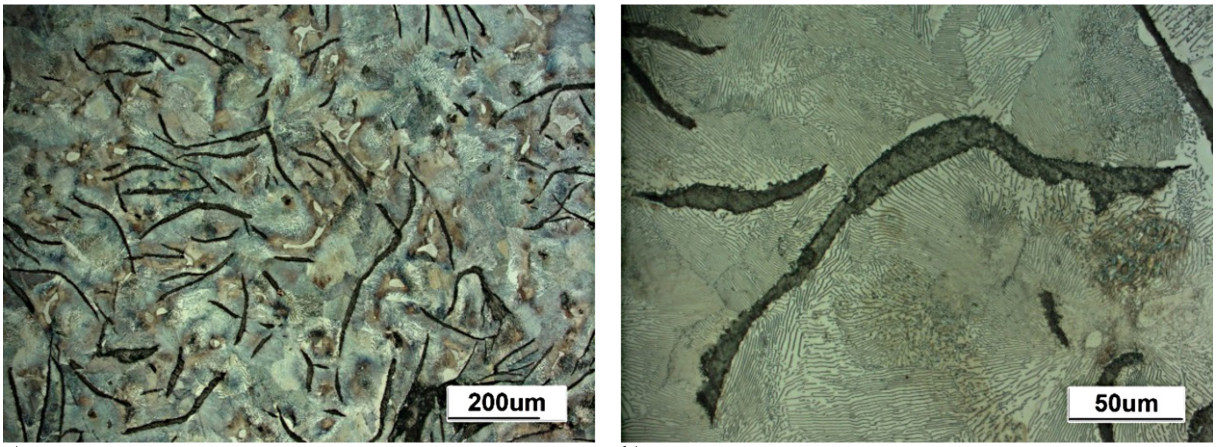

a) b)

Fig. 2. Microstructure of EN-GJL 250 grey cast iron at a) x100; b) x500 magnification

2020-16 tool holder and the TNGN 160408 cutting inserts with a flat rake face. Experimental tests were conducted without and with cooling, where the cooling agent was compressed air.

The structure shown in Fig. 2a–b is typical of grey cast iron. It consists of type A graphite flakes, according to PN EN ISO 945-1 [10], in a metallic perlite matrix with a small amount of ferrite forming the graphite rim.

The chemical composition of the EN-GJL 250 cast iron is shown in Table 1, while the mechanical properties, based on PN-EN 156:2012, are shown in Table 2.

The average hardness of the sample measured at 5 points using the Brinell method, applying a ball indenter with a diameter of 1 mm and a force of 98 N, is 186 HB 1/10.

Table 1. Chemical composition of cast iron EN-GJL 250 [18]

Elements [% by weight]				
C	Si	Mn	P	S
2.8–3.3	1.2–1.7	0.8–1.2	≤ 0.15	≤ 0.12

Table 2. Mechanical properties of cast iron EN-GJL 250 based on PN-EN 156:2012 [11]

Mechanical properties		
Tensile strenght	R_m [MPa]	250–350
Yield strenght	R_e [MPa]	165–228 MPa
Elongation	A [%]	0.8–0.3 %
Modulus of elasticity	E [GPa]	103–118 GPa
Poisson's ratio	ν	0.26
Fracturetoughness	K_{IC}	480

Fig. 3. View of the test bench

Test bench

The experimental tests were carried out on a stand based on a TUM-35D1 centre lathe with a modernized drive system (Fig. 3). During the research, thermographic images were collected separately for all sub-areas of the cutting zone (Fig. 4). For this purpose, the Fluke Tir32 thermal imaging camera from Fluke Thermography, equipped with the SmartViev 4.3 software, was used.

After the end of cutting, the roughness of the processed surface and wear parameters of the cutting tool were measured. Roughness was measured on the MarSurf PS 10 profilographometer, while cutting tool wear was measured on the LEICA MS 5 microscope. The industry most often uses the parameter *Ra* to describe surface roughness. Therefore, in this study, all surface roughness analyses are conducted for this parameter. In the cutting tool wear analysis, the VB_c parameter representing the average width of wear band of the cutting tool corner was selected for comparison. Examples of wear images obtained with a cutting speed v_c= 75 m/min and a cutting time t = 40min are shown in Figure 5. Chip morphology analyses were also conducted on the same microscope.

Turning tests were conducted for the following processing parameters:

- cutting speed, v_c = 50, 75, 100 m/min,
- feed rate, f = 0.20 mm/rev,
- cutting depth, a_p = 1 mm,
- cutting time, t = 20, 40, 60 min.

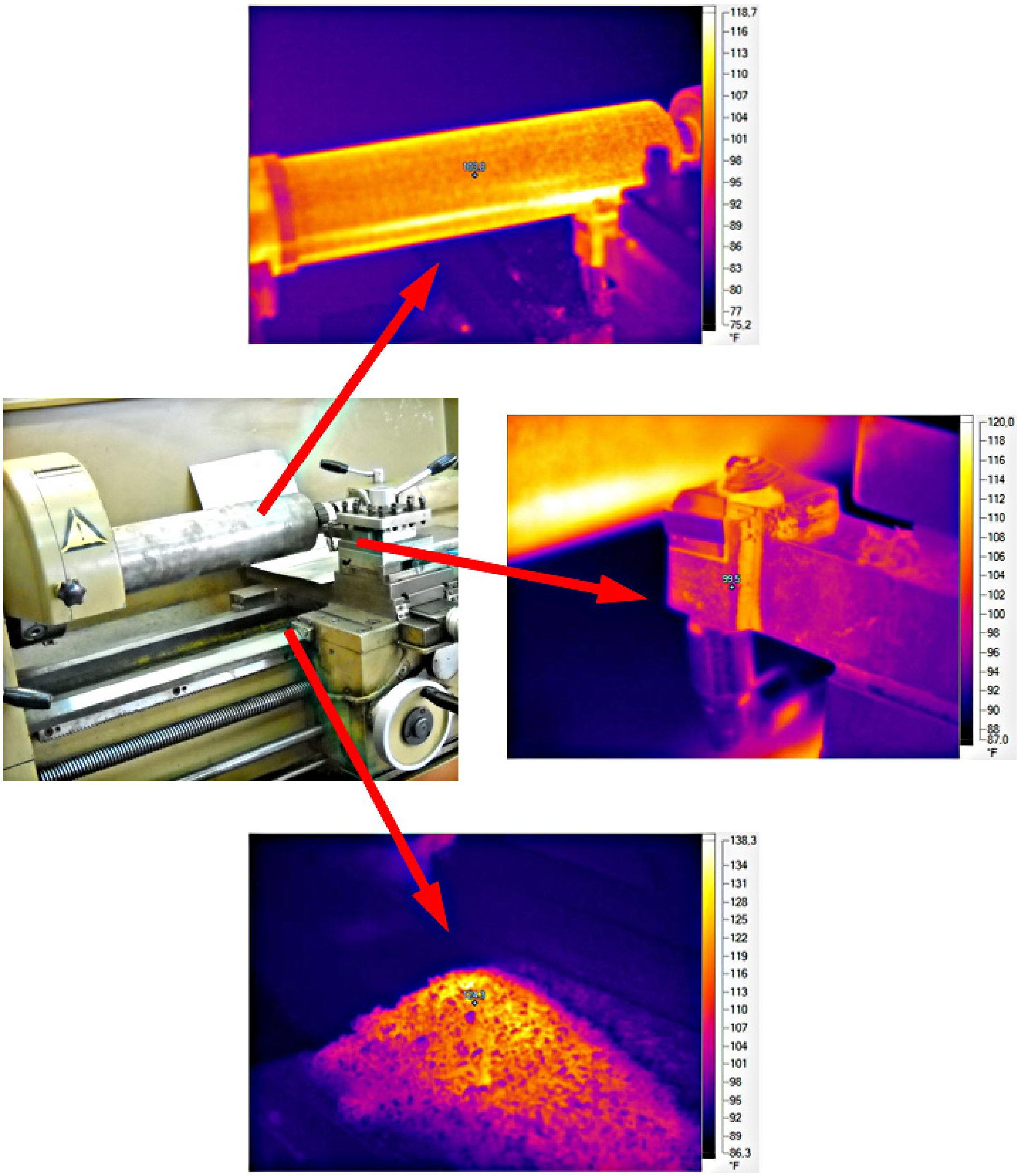

Fig. 4. Location of areas where thermovision measurements were carried out

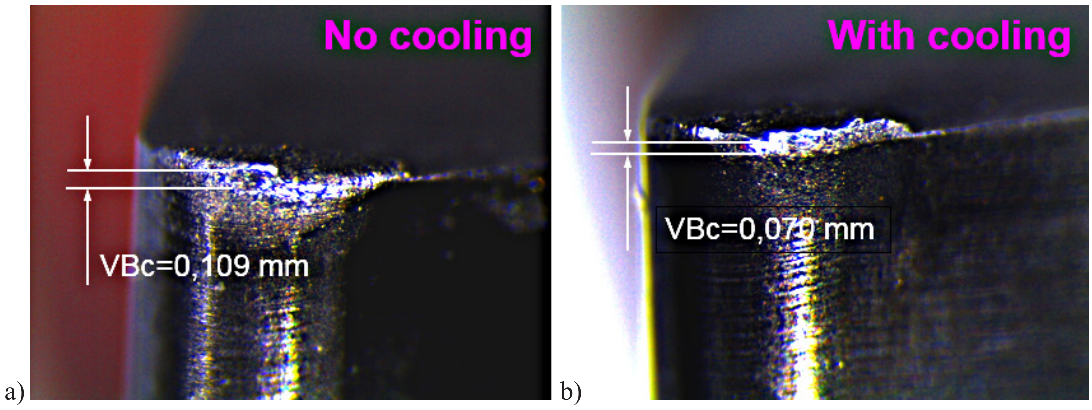

Fig. 5. Comparison of the wear images of the cutting tool corner, a) wear achieved in the absence of cutting tool cooling; b) processing with cutting tool cooling

The machining parameters were selected on the basis of experience gained in the industry and previous research.

Cutting tool cooling system

The cutting tool is cooled using an original system that uses compressed air as the cooling medium. This configuration does not cool down the chip and the chip-cutting tool contact zone, but the bottom of the cutting insert. The idea of this cooling system is schematically shown in Figure 6.

The cooling air under pressure is fed from underneath the cutting tool holder (1) and passes through the axial hole in the screw (7) fixing the support plate (3). In the space above the head of the screw, it expands and escapes to the outside through special channels in the support plate while cooling the bot-tom surface of the cutting insert (5) and support plate (3). The direction of airflow in the figure is indicated by red arrows (6).

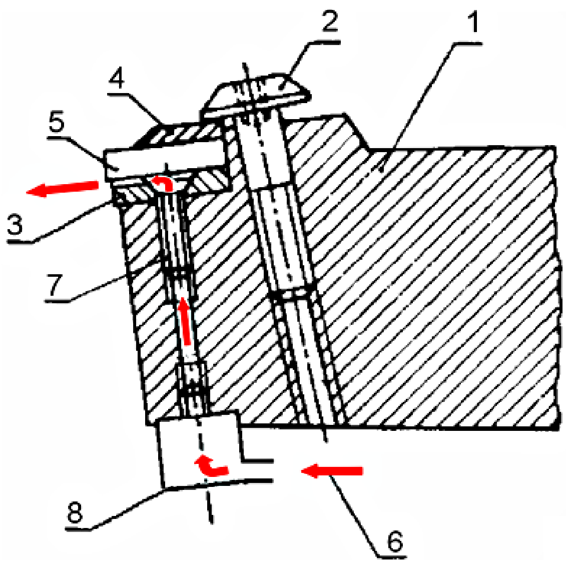

Fig. 6. Diagram of the air cooling system for the cutting tool

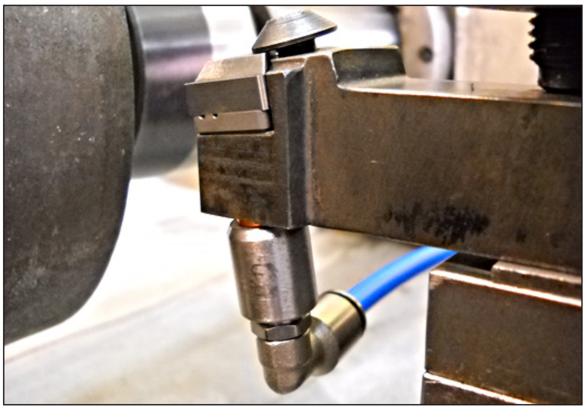

Fig. 7. View of the CTGNR 2020-16 tool adapted for air cooling

For the construction of the cooling system, the CTGNR 2020-16 commercial tool holder was used with only minor modifications:

- execution of a Ø 3 mm through hole in the screw (7) fixing the support plate (3),
- execution of special channels in the support plate (3),
- execution of the air duct connection (8).

The appearance of the complete air cooling system is shown in Figure 7.

The parameters with which cooling was carried out are accordingly:

- air temperature, $Ta = 26$ °C,
- flux $\dot{v} = 0.00029$ m^3/s,
- pressure $p = 0.274$ MPa.

RESULTS AND DISCUSSIONS

The experimental research on the effects of using the air cooling system of the cutting insert from the bottom shows that this method of cooling causes a decrease in temperature in the entire cutting zone. It is obvious that the temperature of the cutting tool shank is reduced. However, there was also a significant reduction in the temperature of the workpiece and chips accumulated on the machine guides, directly under the machining zone. Thermographic images show noticeably lower temperature values of these areas even though they were not directly cooled. This phenomenon can be explained by a change in the distribution of heat fluxes be-tween the cutting tool, chip and workpiece caused by cooling. Cooling of a carbide cutting insert which has a high thermal conductivity (Fig. 1) increases the heat flux entering the tool. This heat is received intensively by a stream of air flowing between the cutting insert and the support plate. The consequence of changing the division of heat fluxes and increased heat dissipation by the cutting insert is a decrease in temperature in all sub-areas of the cutting zone. The comparison of the measured temperature values for cutting with and without cooling is shown in Table 3. The data obtained at a cutting speed of 75 m/min were selected for comparison, as only for this speed no tool vibration or catastrophic cut-ting edge damage was observed.

The course of temperature changes occurring with the change of cutting time in graphic form is shown in Figure 8. You can see there a comparison of temperature values for cutting without and with cooling of the cutting insert recorded for the workpiece material processed at constant cutting parameters and at different processing times.

By analysing the graph, a clear increase in the temperature of the workpiece can be observed, which is proportional to the increase in machining time. However, for cutting with cooling the increase is not as intensive. In the cooling system used, only the cutting insert and not the workpiece was cooled, so the recorded decrease in the workpiece temperature is only caused by changing the distribution of heat fluxes between the chips, cutting tool and workpiece material. It is obvious that the temperature increases shown in the diagram are characteristic of the initial phase of the cutting process and will stabilise after all the system components involved in the heat exchange have heated up. However, already at this stage of work it can be concluded that the application of air cooling of the cutting insert results in a decrease in the temperature of the workpiece by about 22%, of the cutting tool by about 25% and of the chips accumulated on the guide below the cutting zone by about 30%.

The observed lowering of the cutting temperature is a desirable phenomenon, as it translates into reduced cutting tool wear. The wear of the

Table 3. Summary of average temperature values of the observed sub-areas of the cutting zone for the cutting speed of $v_c = 75$ m/min

t, min	T, °C					
	Tool		Workpiece		Chip	
	No cooling	With cooling	No cooling	With cooling	No cooling	With cooling
20	38.8	33.4	33.6	32.3	62.9	48.8
40	57.7	40.3	52.6	39.4	79.0	52.6
60	64.0	44.5	65.0	40.7	89.1	56.5

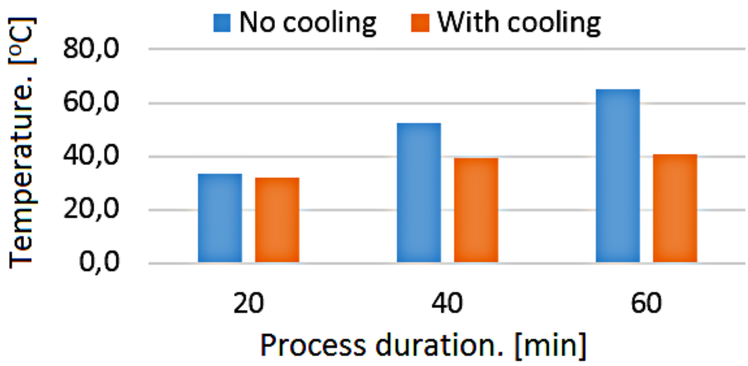

Fig. 8. Average material temperature of the workpiece measured with an IR camera; process parameters $v_c = 75$m/min, $ap = 1$mm, $f = 0.2$mm/rev

Table 4. A comparison of the average values of the VB_C index of cutting tool wear and the *Ra* parameter of surface roughness for turning without and with air cooling

t, min	VB_c		Ra	
	No cooling	With cooling	No cooling	With cooling
20	0.091	0.071	2.964	2.779
40	0.103	0.080	3.171	3.005
60	0.121	0.093	3.249	3.059

cutting tool was measured after each cutting attempt. The study analysed the course of changes in the average width of the wear band of the cutting tool corner VB_C. The average values of this parameter measured at the cutting speed v_c = 75 m/min are shown in Table 4.

Even a cursory analysis of the results shown there indicates that air cooling has measurable effects. The value of the VB_C parameter for cutting with air cooling is on average about 22% lower than the tool wear measured for cutting without cooling.

The change in cutting temperature is also reflected in the roughness of the processed surface. Clearly, a multitude of factors influence surface roughness [12] - even the type of previous treatment [13]. However, these factors were excluded and the considerations focused on estimating the effect of the cooling method on the value of the measured roughness parameter *Ra*. The numerical values of the parameter *Ra* are shown in Table 2. The presented comparison shows that the application of cooling resulted in a reduction of the *Ra* parameter value by about 5.2 to 6.2 %. It is assumed that the reason for these differences is the higher temperature during cutting without cooling. The use of cooling causes the cutting tool to give off much more heat to the environment, thus reducing the temperature in the entire cut-ting zone. As a result, the plasticity of the workpiece material changes and this in turn affects the separation mechanism of the workpiece material.

It might seem that a change in cutting temperature only minimally affects the material separation mechanism and therefore should not be visible in surface roughness measurements. However, a comparison of the roughness profiles and the values of the measured roughness parameters indicates that lowering the cutting temperature significantly changes the decohesion of the material. Specially selected measurements taken at the same processing parameters, for the process with and without cooling, were selected for comparison (Figure 9). The results were chosen so that the *Ra* parameter was comparable in both cases. Even a cursory analysis of the numerical values of the roughness parameters compared shows clear differences. In the case of machining with cooling, a lower value of the *Rz* roughness parameter by more than 13%, a lower value of the maximum surface elevation *Rv* by more than 20%, a lower average value of the *RSm* roughness intervals by more than 24% and a lower coefficient of skewness of the roughness profile *Rsk* by 89% were recorded. At the same time, the value of the reduced elevation of the roughness profile *Rpk* decreased by 23% and the reduced indentation height of the roughness profile *Rvk* by 48%. In addition, there was an increase of more than 10% in the carrying share of the *Mr1* vertices. The results obtained are in line with literature reports, which indicate that an effectively operating cooling system produces workpiece surface roughness [14, 15, 16].

These tests showed unequivocally that the introduction of air cooling of the cutting insert, through a series of tribomechanical interactions, reduced the value of the compared roughness parameter for all the tests carried out.

As previously stated, the air cooling system for the cutting tool used in the research does not cool the chip and cutting zone but cools the bottom surface of the cutting insert. Therefore, such walking has a minimal impact on the morphology of chips. Comparison of the shape of sample chips obtained with a cutting speed v_c = 75 m/min and a cut-ting time t = 40 min are shown in Figure 10.

As you can see, the shape of the chips is very similar in both cases. However, it is noteworthy that the chips produced during cutting with cooling (Figure 10b) have a slightly larger radius of curvature. It is assumed that such a change in chip shape results from a decrease in temperature in the entire cutting zone, including the contact temperature. As a result of lowering the cutting temperature, the chips have a lower temperature gradient, which in turn directly translates into lower chip deformation. A noticeable difference

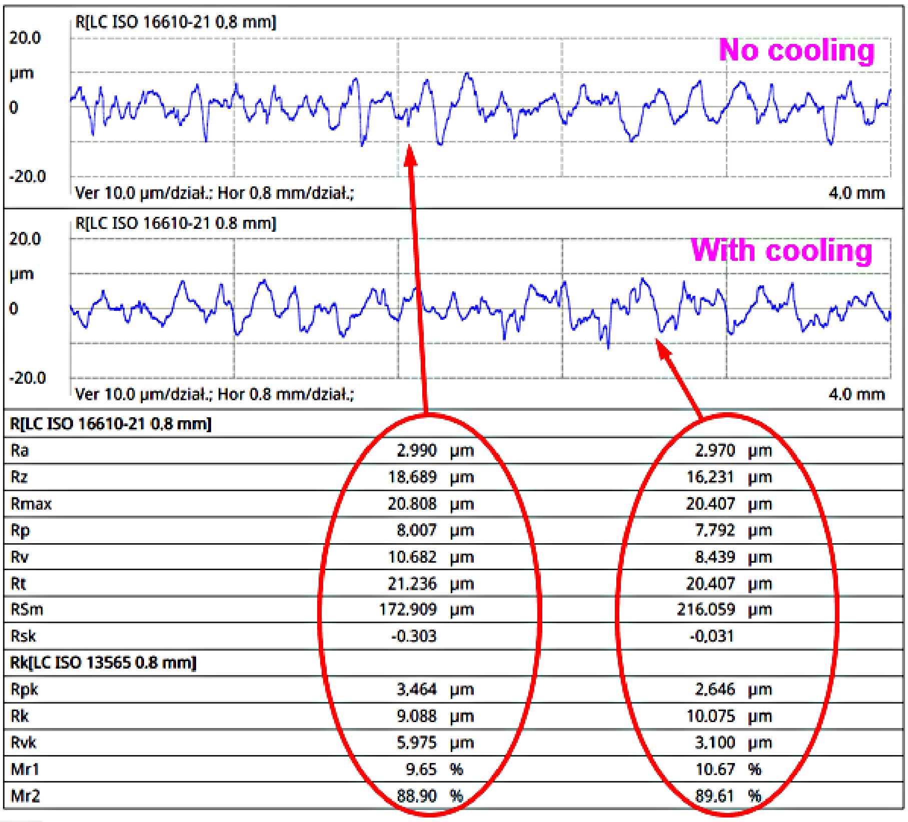

R[LC ISO 16610-21 0,8 mm]		
Ra	2.990 µm	2.970 µm
Rz	18.689 µm	16.231 µm
Rmax	20.808 µm	20.407 µm
Rp	8.007 µm	7.792 µm
Rv	10.682 µm	8.439 µm
Rt	21.236 µm	20.407 µm
RSm	172.909 µm	216.059 µm
Rsk	-0.303	-0,031
Rk[LC ISO 13565 0.8 mm]		
Rpk	3.464 µm	2.646 µm
Rk	9.088 µm	10.075 µm
Rvk	5.975 µm	3.100 µm
Mr1	9.65 %	10.67 %
Mr2	88.90 %	89.61 %

Fig. 9. Comparison of the profile and roughness parameters for turning without and with air cooling, cutting process parameters: v_c = 75 m/min, f = 0.2 mm/rev., ap = 1 mm, t = 20 min

in the observed images is the almost total absence of cast iron dust for chips obtained with cooling (Figure 10b). Such fine metal dust was blown out through the cooling air stream over long distances and was not directly under the tool. The observation shows that this dust settled on the machine's components at a short distance from the cutting tool. From the analysis of the literature conducted in terms of estimating the harmfulness of metal dust produced during mechanical treatment, it is clear that such dust has a very negative impact on the operator's health. It can cause skin diseases and many problems with the respiratory system [8, 17]. Therefore, the use of this type of air cooling system in practice requires caution and health and safety rules to be adhered to.

CONCLUSIONS

The analysis of the results of tests of the air cooling system of the cutting tool which was used during the turning of EN-GJL 250 grey cast iron with TH10 carbide tools, shown in this article,

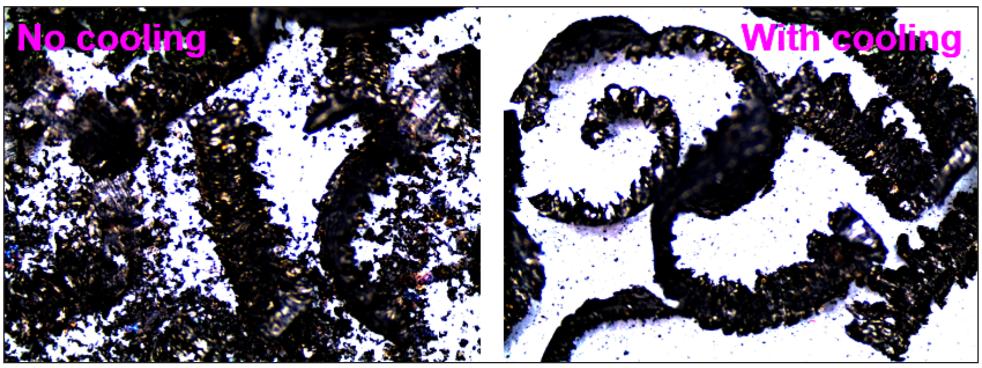

Fig. 10. Comparison of the morphology of chips obtained for cutting: a) without cooling, b) with cooling of the cutting tool. Magnification 9.5 x

allows to formulate the following conclusions. Air cooling of the tool reduces the temperature in the entire cutting zone, including the temperature of the tool by about 25%, the workpiece by about 22% and the chips by about 30%. This way of cooling the cutting tool results in a noticeable reduction in cutting tool wear, as the VB_c parameter for average cutting tool corner wear is reduced by about 22%. Air cooling has a beneficial effect on improving the roughness of the processed surface, as the *Ra* parameter has decreased by about 6%, the *Rz* parameter by more than 13%. The design of the tested carbide insert air cooling system is easy to make, as it requires only minor interventions in the commercial tool holder. The proposed cooling system is universal and can be used on almost every lathe. The analysed method of cooling is ecological because it does not cause environmental pollution with oil emulsion. No costs are incurred for the disposal of used coolants. The disadvantage of such cooling is that metal dust lifted together with cooling air from the cutting zone during machining can be hazardous to the operator's health.

REFERENCES

1. Grzesik W. Advanced Machining Processes of Metallic Materials: Theory, Modelling, and Applications, Elsevier; 2017.
2. Shaw M.C. Metal cutting principles, Oxford University Press; 2004.
3. Davim J.P. (Ed.). Metal Cutting Technologies: Progress and Current Trends, Walter de Gruyter GmbH & Co KG; 2016.
4. Dixit U.S., Sarma A.K., Davim J.P. Environmentally Friendly Machining, Springer; 2012.
5. Quan Y., Mai Q. Investigation of the cooling effect of heat pipe-embedded cutter in dry machining with different thermal conductivities of cutter/workpiece materials and different cutting parameters. International Journal of Advanced Manufacturing Technology. 2015; 79(5): 1161–1169. https://doi.org/10.1007/s00170-015-6889-5
6. Zhu L., Peng S.S., Yin C.L., Jen T.C., Cheng X., Yen Y.H. Cutting temperature, tool wear, and tool life in heat-pipe-assisted end-milling operations. International Journal of Advanced Manufacturing Technology. 2014; 72(5-8): 995-1007. https://doi.org/10.1007 /s00170-014-5699-5
7. Liang L., Quan Y. Investigation of heat partition in dry turning assisted by heat pipe cooling. International Journal of Advanced Manufacturing Technology. 2012; 66(9-12): 1931–1941. https://doi.org/10.1007/s00170-012-4471-y
8. Liang L., Quan Y., Zhiyong K. Investigation of tool-chip interface temperature in dry turning assisted by heat pipe cooling. International Journal of Advanced Manufacturing Technology. 2011; 54(1): 35-43. https://doi.org/10.1007/s00170-010-2926-6
9. Kondej D., Gawęda E. Metals in Dust Fractions Emitted at Mechanical Workstations. International Journal of Occupational Safety and Ergonomics. 2012; 18(4): 453–460. https://doi.org/10.1080/10803548.2012.11076952
10. PN EN ISO 945-1: Cast iron microstructure - Part 1: Classification of graphite precipitates on the basis of visual analysis, 09-20-2019, Polish Committee for Standardization.
11. EN 156:2012 Founding Grey cast iron, Polish Committee for Standardization, 2021, Warsaw, Poland.
12. Ankener W., Uebel J., Basten S., Smaga M., Kirsch B., Seewig J., Aurich J.C., Beck T. Influence of different cooling strategies during hard turning of AISI 52100 – part II: characterization of the surface and near surface microstructure morphology. Procedia CIRP. 2020; 87: 119–124. https://doi.org/10.1016/j.procir.2020.02.094
13. Dhanasekaran P.S., Kalla D.K., Asmatulu R. Human safety problems in industrial machining of composite materials. Composites Manufacturing 2011 Conference and Exhibits. Vol. TP11PUB12. 2011; 1–8.
14. Chuchala D., Dobrzynski M., Pimenov D.Y., Orlowski K.A., Krolczyk G. Surface roughness evaluation in thin EN AW-6086-T6 alloy plates after face milling process with different strategies. Materials. 2021; 14(11): 3036. https://doi.org/10.3390/ma14113036
15. Tanabe I., Yamagami Y., Hoshino H. Development of a New High-pressure Cooling System for Machining of Difficult-to-Machine Materials. Journal of Machine Engineering. 2020; 20(1): 82–97. https://doi.org/10.36897/jme/117776
16. Airao J., Nirala C.K., Bertolini R., Krolczykc G.M., Khanna N. Sustainable cooling strategies to reduce tool wear, power consumption and surface roughness during ultrasonic assisted turning of Ti-6Al-4V. Tribology International. 2022; 169: 107494. https://doi.org/10.1016/j.triboint.2022.107494
17. Nowakowski Ł., Miko E. The analysis of factors impacting the geometrical structure of machined surfaces. Mechanik. 2015; 88(8-9CD2): 11–18. https://doi.org/10.17814/ mechanik.2015.8-9.406
18. The website of the EN-GJL-250 cast iron manufacturer. http://www.iron-foundry.com/en-gjl-250-cast-iron-gg25.html (Access on 07/05/2022)